



Human muscle hardness assessment during incremental isometric contraction using transient elastography

Jean Luc Gennisson^a, Christophe Cornu^{b,c,*}, Stefan Catheline^a,
Mathias Fink^a, Pierre Portero^{b,d}

^a*Ecole Supérieure de Physique Chimie Industrielle, Laboratoire Ondes et Acoustique, CNRS-UMR 7587, 10 rue Vauquelin, 75231 Paris Cedex, France*

^b*Institut de Myologie, Laboratoire de Physiologie Neuromusculaire, GH Pitié-Salpêtrière-47 Bd de l'Hôpital-75013 Paris, France*

^c*UFR STAPS, Laboratoire Motricité, Interactions, Performance (J.E. 2438), 25 bis, bd Guy Mollet, BP 72206, 44322 Nantes cedex 3, France*

^d*Département of STAPS Université Paris XII—Val de Marne, 80 Av du Général de Gaulle, 94010 Créteil, France*

Accepted 19 July 2004

Abstract

The aim of this study was to investigate the relationship between biceps brachii hardness using the transient elastography technique, and its activity level by quantifying the surface electromyographic signal (sEMG). Ten healthy subjects volunteered for this protocol. To assess the maximal biceps brachii myoelectric activity (sEMG-RMSm), subjects had to achieve their maximal voluntary contraction trial during an elbow flexion effort. They were then asked to perform an isometric biceps sEMG-RMS ramp trial in elbow flexion from 0% to 50% of their sEMG-RMSm in 120 s. A low-frequency pulse was sent every 5 s during all trials by an innovative shear elasticity probe previously placed over the belly of the biceps brachii allowing the calculation of a transverse shear modulus. The main results of this study were (i) the finding of a systematic linear relationship between the biceps brachii transverse shear moduli and the corresponding sEMG-RMS values. This was not the case when plotting transverse shear modulus versus the elbow flexion torque production. Therefore, the computation of a hardness index from the slope of individual transverse shear modulus-sEMG-RMS linear relationship was enabled; (ii) It was also found that the higher is the rest shear modulus, the lower is the hardness index, indicating that the transverse shear modulus change during contraction depends on its level at rest. Therefore, this non-invasive technique could be useful in the medical field to explore deep muscles which are unreachable by classical testing methods. It could also be applied for the follow-up of neuromuscular diseases inducing stiffness changes such as in Duchenne muscular dystrophy.

© 2004 Published by Elsevier Ltd.

Keywords: Shear wave; Young's modulus; Isometric contraction; Surface EMG; Muscle hardness

1. Introduction

Viscoelastic properties are observed in both passive and active muscles (Fung, 1993). Muscle stiffness and joint stiffness are important parameters for the control of movement because their levels determine resistance to

external perturbations (Akeson et al., 1987). Moreover, it seems that knowledge of mechanisms responsible for muscle adaptation to changes in functional demand (pathology or training) requires quantification of the mechanical properties of muscle. In fact, muscle contractility and elasticity are sensitive to hyperactivity (e.g. training) as well as hypoactivity (e.g. bed rest). This strengthens the interest in the characterization of such parameters in scientific and medical domains. For instance, elastic properties of a muscle-tendon complex have been previously studied in humans with and without neuromuscular disease using the quick release

*Corresponding author. UFR STAPS, 25 bis, bd Guy Mollet, BP 72206, 44322 Nantes cedex 3, France. Tel.: +33-02-51-83-72-22; fax: +33-02-51-83-72-10.

E-mail addresses: christophe.cornu@staps.univ-nantes.fr, c.cornu@myologie.chups.jussieu.fr (C. Cornu).

technique (Goubel and Pertuzon, 1973; Pousson et al., 1990; Cornu et al., 1998, 2001, 2003; Cornu and Goubel 2001; Hof 1998; Zee and Voigt, 2001).

Another widely used approach for determining the elastic properties of joints involves generating sinusoidal perturbations over a range of frequencies (Joyce et al., 1974; Zahalak and Heyman, 1979; Winters et al., 1988; Cornu et al., 1997, 2001; Lambertz et al., 2001).

However, all these methods are very useful for the understanding of human movements but they only provide global measure for describing the behavior of a muscle and/or joint system. Some methods, for instance the use of ultrasonic waves, allow the mechanical characterization of specific structures such as tendon (Kubo et al., 2001). Such methods allow the study of specific structure's behavior within a muscle–tendon complex. However, those investigations are limited to superficial structures.

Furthermore, all the above studies concern the assessment of the musculo-tendinous complex stiffness among the longitudinal axis. Another approach is the characterization of a transverse muscle stiffness that has been termed hardness (Murayama et al., 2000).

In fact, it is well-known from palpation that muscle becomes harder in some physiological conditions, e.g., voluntary contraction and in pathological conditions such as spasm, cramps, oedema and delayed onset muscle soreness. Nevertheless, few studies have quantified hardness changes in normal and pathological conditions. Murayama et al. (2000), using an eccentric exercise protocol which induced muscle stiffness and swelling, have shown an increase in muscle hardness assessed by a pressure method. Ultrasonic methods have also been proposed to quantify hardness changes. Quantitative induced motion (using a low-frequency vibrator) obtained with Doppler techniques allows one to estimate the Young's modulus of soft tissues (Krouskop et al., 1987; Yamakoshi et al., 1990; Lerner et al., 1988). Applied on human quadriceps muscle, these techniques showed that the Young's modulus was highly correlated to the muscle contraction level (Levinson et al., 1995). In transient elastography, the applied monochromatic vibrations are replaced by a low-frequency (50–500 Hz) pulse (Catheline et al., 1999). The displacements are calculated from a speckle tracking method (Ophir et al., 1991). Thus, the energy propagates within isotropic soft tissues as compressional (P) and shear (S) waves with typical velocities of $V_P = 1500 \text{ m.s}^{-1}$ and $V_S = 2 \text{ m.s}^{-1}$, respectively. Since the muscles are anisotropic (Levinson, 1987) these velocities depend upon the direction of the propagation and on the polarization of the waves. In the biceps where the fibers are all aligned on the same axis (transverse isotropy), the study of shear wave propagation in the direction perpendicular to the fibers is simplified. The speeds of two shear waves with a

polarization perpendicular and parallel to the fibers, are given, respectively, by

$$V_s^\perp = \sqrt{\frac{c_{66}}{\rho}}, \quad V_s^\parallel = \sqrt{\frac{c_{44}}{\rho}}. \quad (1)$$

c_{44} and c_{66} stands for the elastic coefficients of the Christoffel's matrix in Voigt's notation and ρ for the density. The shear elasticity cannot be assessed using ultrasounds because they only deal with bulk elasticity. It has been shown (Gennisson et al., 2003) that the use of a rod piston is needed in order to control the polarization of the shear waves with transient elastography technique. Thus, the general idea is that measuring the speed of shear waves allows one to deduce an elastic coefficient given that ρ is fixed (in muscle, $\rho \approx 1000 \text{ kg.m}^{-3}$). In this paper, a more sophisticated approach is used to measure the elasticity: the inverse problem. However, in this study we only focused on the examination of c_{66} , the shear modulus. The main objective of this study was to characterize biceps brachii transversal hardness index using the elastographic method and to determine whether it was related to local muscle activation changes during an incremental standardized isometric contraction.

2. Materials and methods

2.1. Subjects

Ten healthy subjects (mean age: 26.8 ± 3.2 years; mean height: 175.7 ± 6.2 cm; mean weight: 69.5 ± 9.0 kg) volunteered for this study. All subjects were informed of the nature and aim of this study. They signed an informed consent form.

2.2. Materials

2.2.1. Local hardness assessment

The local hardness assessment is obtained with the shear elasticity probe (Sandrin et al., 2002a,b) shown in Fig. 1a. The ultrasonic transducer (7 mm diameter and 35 mm focal depth) is set up in the middle of a rod ($3 \times 80 \text{ mm}^2$) on a vibrator (Brüel & Kjær, type 4810). A pulse echo system is used with a 2 kHz recurrence frequency. The ultrasonic signals (5 MHz central frequency) are sampled at 50 MHz and stored using a 9-bit digitizer with 2 Mbytes memory. The shear elasticity probe is applied at the surface of the biceps and the rod indicates the direction of the elbow–shoulder axis (Fig. 1b).

A typical ultrasonic signal is represented in Fig. 2a. Two main zones emerge from the muscular fibers echoes. They correspond to the biceps and the agonist. One sinusoid cycle (150 Hz) from a function generator is sent to the vibrator. This pulse propagates within

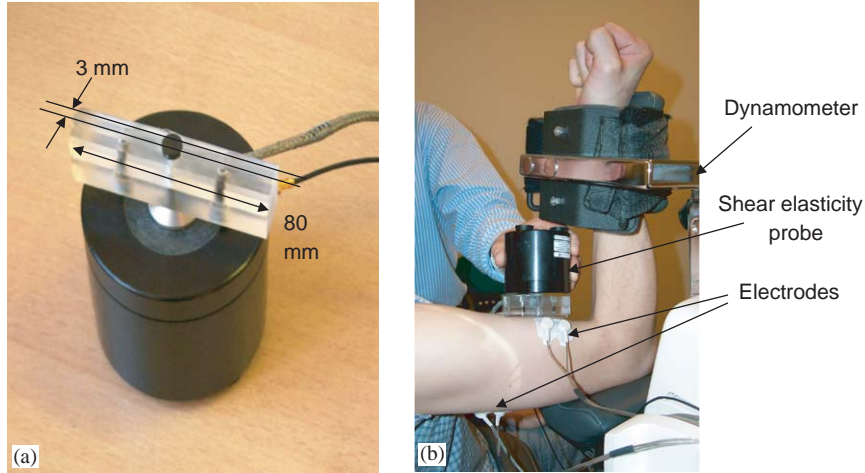


Fig. 1. (a) The shear elasticity probe. (b) The local shear modulus is measured from the shear wave displacements induced by a low-frequency pulse sent in the biceps brachii.

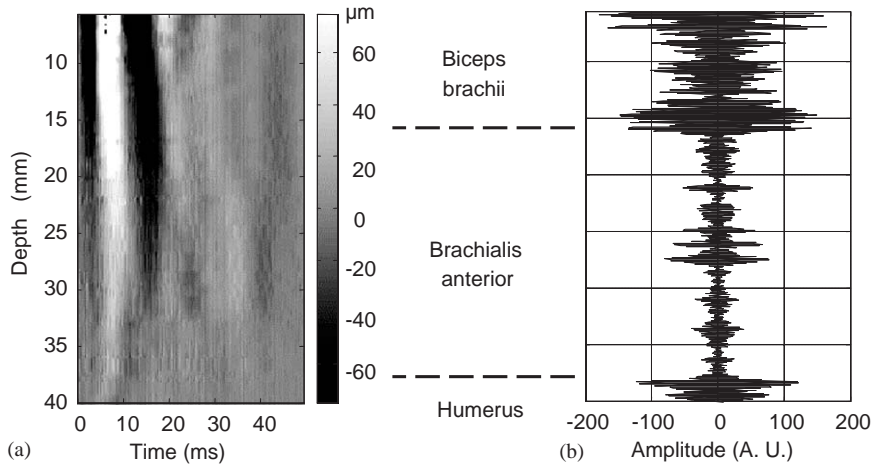


Fig. 2. (a) Gray-scale image of the experimental displacement as a function of the depth and time obtained for an acoustic pulse (150 Hz) in the anterior part of the arm. (b) Ultrasonic signal on the arm as a function of the depth (or time of flight). The same depth scale is used in (a) and (b). Three different zones are clearly visible on the ultrasonic signal: the biceps brachii, the brachialis anterior and the humerus.

muscles as a shear wave. The detection of the motion induced by such a wave is carried out with a cross-correlation technique on backscattered ultrasonic signal stored in memory. A typical displacement field (Fig. 2b) is represented on a gray-scale level as a function of time and depth.

From the displacement field, the transverse shear elastic constant c_{66} is computed using an inversion algorithm. The inverse problem algorithm is based on a simplified approach of the direct problem. The most general form of the wave equation in linear elastic medium can be expressed as (Brekhovskikh and Godin, 1990)

$$\rho_0 \frac{\partial^2 u_i}{\partial t^2} - \frac{\partial}{\partial x_j} \left(c_{ijkl} \frac{\partial u_l}{\partial x_k} \right) = S(\vec{r}, t), \quad (2)$$

where u_i is the displacement component, ρ_0 the density, c_{ijkl} the Christoffel's matrix and $S(\vec{r}, t)$ is the source term.

$S(\vec{r}, t) = 0$, in the situation where no source is present in the investigated volume.

In the case of muscle, the wavelength (a few centimeters for shear waves and a few meters for compression waves) is much bigger than the muscular fibers. Thus the medium is considered as homogeneous and Eq. (2) becomes:

$$\rho_0 \frac{\partial^2 u_i}{\partial t^2} = c_{ijkl} \frac{\partial^2 u_l}{\partial x_k \partial x_j}. \quad (3)$$

Since the anisotropy of muscle is properly described by the hexagonal system, the Christoffel's tensor, for a propagation direction perpendicular to the muscle fibers, only contains three elastic constants c_{11} , c_{44} , c_{66} that are involved in the propagation of a longitudinal wave and two shear waves, respectively. In the experiment, the distance propagation under investigation (along the ultrasonic beam) is smaller than the rod

length. Since the rod source is placed in the direction of the elbow–shoulder axis, for symmetry reasons, the problem is reduced to the transverse isotropic plane (perpendicular to the fibers).

$$\rho_0 \frac{\partial^2 \vec{u}}{\partial t^2} = (c_{11} - c_{66}) \vec{\nabla} \vec{\nabla} \vec{u} + c_{66} \nabla^2 \vec{u}. \quad (4)$$

From an experimental point of view, the longitudinal wave can be neglected in the particular case of a pulsed excitation as it propagates instantaneously regarding to the shear wave. Thus, Eq. (4) can be reduced to a simple equation involving one elastic coefficient c_{66} :

$$\rho_0 \frac{\partial^2 \vec{u}}{\partial t^2} = c_{66} \nabla^2 \vec{u}. \quad (5)$$

As the displacement estimation is based on a 1D correlation algorithm, only displacements along the ultrasonic beam axis can be measured. Thus, one can only rely on the z -component of the displacement vector. For this reason, the basic equation used in the inversion algorithm is reduced to

$$\rho_0 \frac{\partial^2 u_z}{\partial t^2} = c_{66} \Delta u_z, \quad (6)$$

where the Laplacian term in the isotropic transverse plane is given by

$$\Delta u_z = \frac{\partial^2 u_z}{\partial x^2} + \frac{\partial^2 u_z}{\partial z^2}. \quad (7)$$

One last approximation is needed. Indeed, the second-order derivative in x cannot be experimentally estimated. Fortunately, with a numerical simulation based on Green's functions, it has been shown (Gennisson, 2003) that the following assumption can be made:

$$\frac{\partial^2 u_z}{\partial x^2} \ll \frac{\partial^2 u_z}{\partial z^2}. \quad (8)$$

This inequality expresses that the shear wave is locally plane. Thus, the Laplacian is reduced to the second-order derivative in z and the wave equation can be reduced to

$$\rho_0 \frac{\partial^2 u_z}{\partial t^2} = c_{66} \frac{\partial^2 u_z}{\partial z^2}. \quad (9)$$

Using this equation (Eq. (9)), it is easy to locally estimate the shear modulus in the medium at each time step:

$$c_{66}(z, t) = \rho_0 \frac{\partial^2 u_z(z, t) / \partial t^2}{\partial^2 u_z(z, t) / \partial z^2}. \quad (10)$$

A higher signal-to-noise ratio can be obtained in the Fourier domain. Then, the shear modulus defined in equation (Eq. (11)) can be expressed as a function of the

Laplacian and displacement Fourier transform (FT):

$$c_{66} \approx \frac{\rho_0}{N_\omega \cdot N_z} \sum_{i=1}^{N_\omega} \sum_{j=1}^{N_z} \frac{|\omega_i^2 FT(u_z(z_j, t))|}{|FT\left(\frac{\partial^2 u_z(z_j, t)}{\partial z^2}\right)|}, \quad (11)$$

where N_ω , N_z correspond to the number of significant discrete frequencies and to the number of depth step within the biceps.

2.2.2. Muscle strength and sEMG data assessment

A Biodex[®] dynamometer (validated by Taylor et al., 1991) was used in this study. This dynamometer is composed of three parts: a servomotor unit, a control unit (panel and software), and a movable seat. Furthermore, specific software (PROTAGS[®]) developed in our laboratory was used to record mechanical data (torque, velocity, angle), surface electromyographic (sEMG) signals and the trigger signal from the shear elasticity probe shots. Using visual feedback, this software allowed the subject to follow a linear sEMG-RMS ramp. This software was also utilized in the analysis of these data. The ramp was set to a level of sEMG-RMS and to a time duration, both established by the examiner. Lastly, silver chloride surface electrodes (4 mm diameter), with an interelectrode (center-to-center) distance of 11 mm, were used to record sEMG activity of elbow muscles during testing (Fig. 1b). sEMG signals were amplified with a frequency bandwidth ranging from 10 to 1000 Hz and were band-pass filtered (6–500 Hz) with a Gould[®] amplifier (6600).

Mechanical and myoelectrical data were processed using PROTAGS[®]. For each impulsive shot, the software determined the biceps brachii (BB) and triceps brachii (TB) levels of sEMG-RMS and the level of torque. Those data were then correlated to the biceps hardness determined with the shear elasticity probe. For the sEMG signals, RMS values were calculated on windows of 250 ms without overlapping during the ramp trial. In the first second of the trial, subjects were asked to relax so the sEMG-RMS signal determined during the first 250 ms window was considered as noise and systematically subtracted from the following calculated sEMG-RMS values.

2.3. Protocols

Surface electrodes were placed on the biceps brachii and on the antagonist muscle, i.e. the triceps brachii. Electrode position corresponded to SENIAM project recommendations. Low impedance at the skin–electrode surface was obtained ($Z < 2 \text{ k}\Omega$) by abrading the skin and cleaning with alcohol. The subjects upper arm was then placed in a 90° flexion position. The distal part of the upper arm was resting on a fixed support. The angle between the upper-arm and the forearm was set to 90° in a para-sagittal plane. A strap attached the forearm to

the dynamometer lever arm at the level of the wrist that was placed in a semi-prone position. The rotation axis of the elbow joint was visually aligned with the rotation axis of the dynamometer. Moreover, straps were positioned across the chest, pelvis and mid-thigh to minimize torso, hip and thigh motion during the contraction. Following a specific warm-up consisting of learning the task of elbow flexion incremental effort, three trials of maximal voluntary contraction (MVC) in an isometric condition were performed. The maximum MVC was retained as the daily MVC of the subjects and allowed to calculate the corresponding maximal root mean square (sEMG-RMSm) of the biceps brachii. Then, two isometric linear sEMG-RMS ramps of 120 s were performed using an instantaneous visual feedback from 0% to 50% of the biceps sEMG-RMSm previously determined. Before the ramp test, the subject was asked to stay at rest during 2 s. Moreover, an incomplete ramp was first performed in order to familiarize the subject to the sEMG-RMS feedback and to control the feasibility of the test. A 2 min rest interval was provided between each trial.

Before each ramp trial, the shear elasticity probe was applied at the surface of the biceps. The rod was parallel to the shoulder–elbow axis and a low-frequency pulse was sent every 5 s during the 120 s contraction. For each acquisition the transverse shear modulus was calculated.

2.4. sEMG-RMS-shear modulus relationship

For all subjects, the sEMG-RMS and the elasticity modulus values were assessed at each impulse. They were normalized with the sEMG-RMSm value and the shear elasticity value at rest, respectively. Then, these normalized data were plotted together, describing a

linear relationship that allowed the determination of a stiffness index which is the slope of the modulus-biceps sEMG-RMS. This index characterizes the subject biceps hardness.

2.5. Statistical analysis

A regression analysis was performed using Sigma-Stat[®] software. For all mechanical and myoelectrical parameters, results are presented as means \pm standard error. For all tests, the level of significance was established at $p < 0.05$.

3. Results

Typical raw data obtained during a ramp trial are presented in Fig. 3 and lead to the results presented in Fig. 4. These results show a linear increase of biceps brachii sEMG-RMS without any triceps brachii co-contraction. These results are also associated with a non-linear increase of flexors torque production with time. Furthermore, the biceps brachii shear modulus also describes a linear increase with respect to time.

When considering each individual's data, a non-linear relationship is systematically observed between biceps brachii sEMG-RMS and flexors torque production (Fig. 5). When plotting data for all subjects (degree of freedom = 286), a global linear relationship is found between the normalized biceps brachii sEMG-RMS and shear modulus. This leads to a global hardness index (slope of the relationship) of 2.34 ± 0.30 ($r^2 = 0.17$, $p < 0.05$). In fact, the individual biceps brachii sEMG-RMS—shear modulus normalized relationships systematically show a linear shape ($p < 0.05$). The slope of the

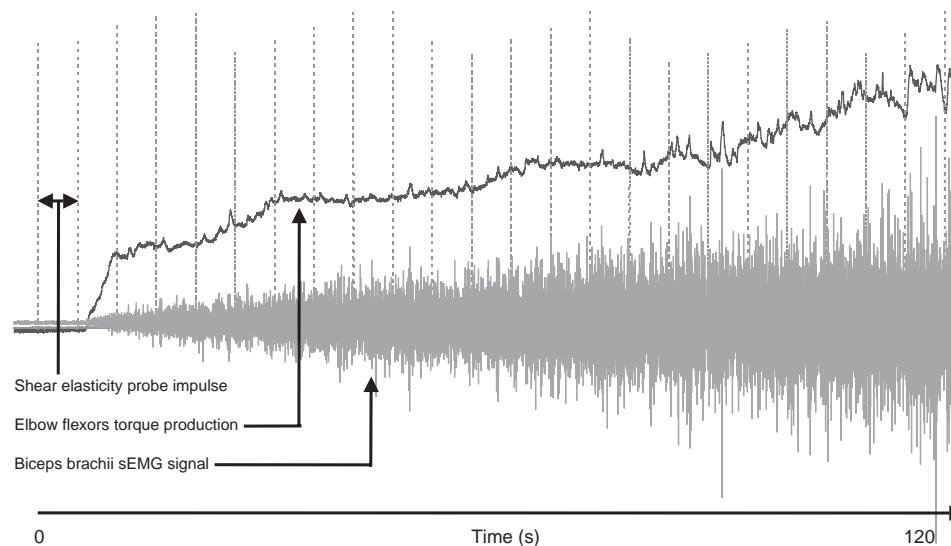


Fig. 3. Typical raw data obtained during an isometric contraction from a linear biceps brachii sEMG-RMS ramp trial. A trial lasted for 2 min and the impulse shots were performed every 5 s. The torque developed at the end of the ramp by the subject was 29.75 N m corresponding to 41% MVC.

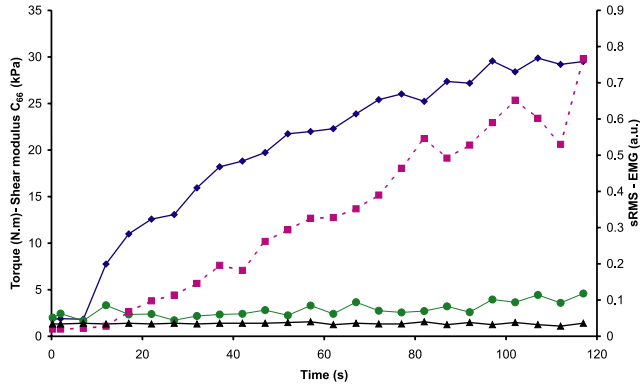


Fig. 4. Typical raw results calculated during an isometric contraction from a linear biceps sEMG-RMS ramp trial. ■: biceps brachii sEMG-RMS; ▲: triceps brachii sEMG-RMS; ◆: flexors torque production; ●: biceps brachii shear modulus (c_{66}).

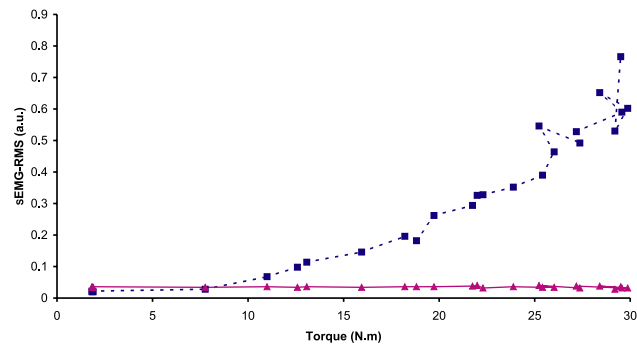


Fig. 5. Typical sEMG-RMS versus flexors torque relationships. ■: biceps brachii sEMG-RMS; ▲: triceps brachii sEMG-RMS.

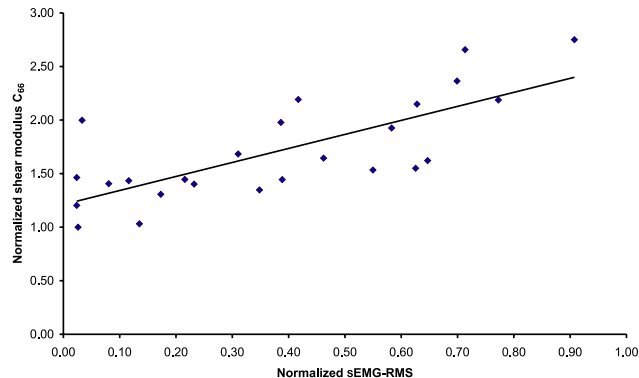


Fig. 6. Typical individual biceps brachii sEMG-RMS—shear modulus normalized relationship. The shear modulus c_{66} is normalized versus the rest shear modulus and the sEMG-RMS versus its maximum value. A hardness index (1.31 ± 0.22) is calculated as the slope of this linear relationship ($r^2 = 0.55$, $p < 0.05$).

relationship corresponds to the hardness index (Fig. 6). Mean hardness index is found to be 3.08 ± 2.20 and the individual values presented in Table 1 range between 1.22 and 8.01 ($p < 0.05$).

Moreover, mean rest biceps brachii hardness was found to be 0.92 ± 0.55 kPa (Table 1). A relationship was obtained plotting rest shear modulus versus hardness

Table 1

Individual hardness index and rest shear modulus values

Subjects	Hardness index	Rest shear modulus (kPa)
1	1.31	1.21
2	1.83	0.75
3	1.35	1.67
4	8.01	0.33
5	2.89	0.37
6	4.54	0.42
7	1.22	1.30
8	1.45	1.65
9	3.41	1.23
10	4.81	0.32
Mean	3.08	0.92
SD	2.20	0.55

SD: standard deviation.

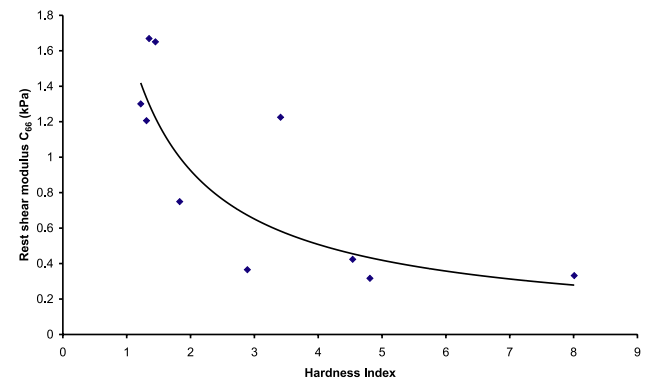


Fig. 7. Hardness index—rest shear modulus relationship. The best fit consists in a power function showing an decrease of biceps brachii hardness index values when its rest shear modulus c_{66} increases ($r^2 = 0.69$, $p < 0.05$).

index. It shows that the higher the rest modulus the lower the hardness index (Fig. 7, $r^2 = 0.69$, $p < 0.05$). This means that the weaker is the elasticity at rest, the more prominent is the variation of elasticity.

4. Discussion

The present experiment was designed in order to determine in vivo muscle hardness during a standardized isometric muscle contraction. This was performed using an innovative tool allowing local muscle hardness evaluation. An original protocol, based on sEMG-RMS feedback, was also designed to be sure that the tested muscle was activated progressively as isometric elbow flexor torque increased. This allowed us to correlate two local muscle parameters, biceps brachii sEMG-RMS and hardness index, rather than a more global parameter such as elbow torque production and a muscle hardness index. In fact, a non-linear relationship between torque production and biceps brachii

sEMG-RMS was found showing that this relationship is influenced by other agonistic muscles that contribute to elbow flexion torque production without any control of their sequence and level of activation. Hence, the interpretation of such results is somewhat difficult (Grabiner et al., 1988; Hunter and Enoka, 2001).

The shear modulus assessment presented in this paper is in accordance with the literature, although some improvements on the elastography protocols can be considered. Indeed, the mean shear wavelength is influenced by the biceps size and shape. Hence, the changing boundaries may influence the shear modulus measurements. One solution to counter this effect is to use a robust vibrator able to generate higher-frequency shear waves that are strongly attenuated. Another difficulty arises from the positioning of the shear elasticity probe. The use of a mechanical lever controlled by a pressure transducer between the probe and the biceps would improve the reproducibility of the measurements. This problem was controlled here by the manipulator. In the literature, rest shear modulus ranges from 12 kPa with a Doppler technique (Levinson et al., 1995; Fujii et al., 1994) to 24 kPa with MRI (Dresner et al., 2001). These values are higher than the mean rest shear modulus shown in Table 1, $\bar{c}_{66} = 0.92$ kPa. Two main reasons explain this difference. First, Levinson and Fujii's assessments were obtained on a different muscle: the quadriceps. Second, Dresner studied the shear wave propagating along the biceps fibers which means that these measurements quantify the longitudinal shear modulus (c_{44}) instead of the transverse shear modulus (c_{66}). Nevertheless the above authors found an increasing global Young's modulus with an increasing mechanical solicitation of a musculo-tendinous complex (involving several muscles) which is in general agreement with our measurements. In the present paper, two main aspects of these experiments have been refined due to the shear elasticity probe: (i) the current study deals with the activity of an isolated muscle (biceps brachii); (ii) because its anisotropic properties, several elastic moduli completely define the muscle elastic behavior. The transverse shear modulus alone (c_{66}) is characterized here.

Our results show a non-linear increase of torque production during the isometric linear sEMG-RMS ramp which illustrates the role played by agonistic muscles, notably at the beginning of an isometric ramp contraction. It also could be asserted that the global muscle transversal section increases due to contraction of those agonistic muscles. These agonistic muscles influence the biceps brachii hardness and induce a compression in the anterior arm compartment. Nevertheless, these compression effects seem to be limited in the characterization of muscle transversal hardness since a linear relationship is systematically found between this parameter and biceps brachii sEMG-RMS.

The increase in muscle hardness parallels the muscle activation. Hence, the transversal muscle hardness changes during contraction could be attributed to structural modifications. Namely the progressive tension on myofilaments, due to contractile protein longitudinal movement, leads to an increase in the transversal section and also to an increase in intramuscular pressure as the muscle is placed in a closed volume. In fact, Korner et al. (1984) found that the sEMG signals from the biceps brachii and the intramuscular pressure were always correlated during isometric contraction. Jarvholm et al. (1991), who worked on shoulder muscles, also showed that both sEMG and intramuscular pressure were correlated to isometric external force whatever the tested muscle. Finally, Davis et al. (2003) observed a good correlation between rabbit tibialis anterior muscle force and intramuscular pressure.

Shear modulus hardness changes parallel biceps brachii sEMG-RMS which allows the determination of a hardness index parameters independent of the level of contraction. In fact, hardness index shows inter-individual differences. These differences seem to characterize the subjects since no relationship was found between either body weight or the body mass index and the hardness index. Furthermore, it has been shown that the lower the hardness index is at rest, the higher the muscle hardness increases during contraction. Since subjects reach the same level of contraction (50% biceps brachii sEMG-RMS value), this shows that muscle hardness is partially due to contraction mechanisms but also to muscle spatial adjustment during the contraction.

This kind of normalized parameter may be very useful to follow-up the effects of a neuromuscular pathology, a therapeutic treatment or a rehabilitation protocol since muscle stiffness changes often occur with induced changes in muscle functional demand. Moreover, this non-invasive technique could allow one to assess the local activity of deep muscles unreachable by classical hardness characterization testing methods. Future work should include other elastic coefficients study such as c_{44} , as well as viscosity assessment.

Acknowledgements

The authors would like to thank Peter McNair, Marie-Ange Janvier, François Yu and Marie-Hélène Roy Cardinal for editing the English.

References

- Akeson, W.H., Amiel, D., Abel, M.F., Garfin, S.R., Woo, S.L., 1987. Effects of immobilization on joints. *Clinical Orthopaedics and Related Research* 219, 28–37.
- Brekhovskikh, L.M., Godin, O.A., 1990. *Acoustics of Layered Media I: Plane and Quasi-Plane Waves*. Springer, Berlin.

- Catheline, S., Wu, F., Fink, M., 1999. A solution to diffraction biases in sonoelasticity: the acoustic impulse technique. *Journal of Acoustical Society of America* 105, 2941–2950.
- Cornu, C., Goubel, F., 2001. Musculo-tendinous and joint elastic characteristics during elbow flexion in children. *Clinical Biomechanics* 16, 758–764.
- Cornu, C., Almeida Silveira, M.I., Goubel, F., 1997. Influence of plyometric training on the mechanical impedance of the human ankle joint. *European Journal of Applied Physiology* 76, 282–288.
- Cornu, C., Goubel, F., Fardeau, M., 1998. Stiffness of knee extensors in Duchenne muscular dystrophy. *Muscle and Nerve* 21, 1772–1774.
- Cornu, C., Goubel, F., Fardeau, M., 2001. Muscle and joint elastic properties during elbow flexion in Duchenne muscular dystrophy. *Journal of Physiology* 533, 605–616.
- Cornu, C., Maisetti, O., Ledoux, I., 2003. Muscle elastic properties during wrist flexion and extension in healthy sedentary subjects and volley-ball players. *International Journal of Sports Medicine* 24, 277–284.
- Davis, J., Kaufman, K.R., Lieber, R.L., 2003. Correlation between active and passive isometric force and intramuscular pressure in the isolated rabbit tibialis anterior muscle. *Journal of Biomechanics* 36, 505–512.
- Dresner, M.A., Rose, G.H., Rossman, P.J., Muthupillai, R., Manduca, A., Ehman, R.L., 2001. Magnetic resonance elastography of skeletal muscle. *Journal of Magnetic Resonance Imaging* 13, 269–276.
- Fujii, K., Sato, T., Kameyama, K., Inoue, I., Yokoyama, K., Kobayashi, K., 1994. Imaging hardness distribution in soft tissue in vivo using forced vibration and ultrasonic detection. *Acoustical Imaging Proceeding* 21, 253–258.
- Fung, Y.C., 1993. *Biomechanics, Mechanical Properties of Living Tissues*. 2nd ed. Springer, New York, pp. 392–424.
- Gennisson, J.L., 2003. The shear elasticity probe: a new tool for biological soft tissue investigation. Ph.D. Thesis, Paris VI University, France.
- Gennisson, J.L., Catheline, S., Chaffai, S., Fink, M., 2003. Transient elastography in anisotropic medium: Application to the measurement of slow and fast shear wave velocities in muscles. *Journal of Acoustical Society of America* 114, 536–541.
- Goubel, F., Pertuzon, E., 1973. Evaluation de l'élasticité du muscle in situ par une méthode de quick-release. *Archives Internationales de Physiologie, de Biochimie et de Biophysique* 81, 697–707.
- Grabiner, M.D., Robertson, R.N., Campbell, K.R., 1988. Effects of fatigue on activation profiles and relative torque contribution of elbow flexor synergists. *Medicine and Science in Sports and Exercise* 20, 79–84.
- Hof, A.L., 1998. In vivo measurement of the series elasticity release curve of human triceps surae muscle. *Journal of Biomechanics* 31, 793–800.
- Hunter, S.K., Enoka, R.M., 2001. Sex differences in the fatigability of arm muscles depends on absolute force during isometric contractions. *Journal of Applied Physiology* 91, 2686–2694.
- Jarvholm, U., Palmerud, G., Karlsson, D., Herberts, P., Kadefors, R., 1991. Intramuscular pressure and electromyography in four shoulder muscles. *Journal of Orthopaedic Research* 9, 609–619.
- Joyce, G.C., Rack, P.M., Ross, H.F., 1974. The forces generated at the human elbow joint in response to imposed sinusoidal movements of the forearm. *Journal of Physiology* 240, 351–374.
- Korner, L., Parker, P., Almstrom, C., Andersson, G.B., Herberts, P., Kadefors, R., Palmerud, G., Zetterberg, C., 1984. Relation of intramuscular pressure to the force output and myoelectric signal of skeletal muscle. *Journal of Orthopaedic Research* 2, 289–296.
- Krouskop, T.A., Dougherty, D.R., Vinson, F.S., 1987. A pulsed Doppler ultrasonic system for making noninvasive measurements of the mechanical properties of soft tissue. *Journal of Rehabilitation Research* 24, 1–8.
- Kubo, K., Kanehisa, H., Fukunaga, T., 2001. Is passive stiffness in human muscles related to the elasticity tendon structure? *European Journal of Applied Physiology* 85, 226–232.
- Lambertz, D., Pérot, C., Kaspranski, R., Goubel, F., 2001. Effects of long-term spaceflight on mechanical properties of muscles in humans. *Journal of Applied Physiology* 90, 179–188.
- Lerner, R.M., Parker, K.J., Holen, J., Gramiak, R., Waag, R.C., 1988. Sonoelasticity: Medical elasticity images derived from ultrasound signals in mechanically vibrated targets. *Acoustical Imaging* 16, 317–327.
- Levinson, S.F., 1987. Ultrasound propagation in anisotropic soft tissues: The application of linear elastic theory. *Journal of Biomechanics* 20, 251–260.
- Levinson, S.F., Shinagawa, M., Sato, T., 1995. Sonoelastic determination of human skeletal muscle elasticity. *Journal of Biomechanics* 28, 1145–1154.
- Murayama, M., Nosaka, K., Yoneda, T., Minamitani, K., 2000. Changes in hardness of the human elbow flexor muscles after eccentric exercise. *European Journal of Applied Physiology* 82, 361–367.
- Ophir, J., Céspedes, I., Ponnekanti, H., Yasdi, Y., Li, X., 1991. Elastography: a quantitative method for imaging the elasticity of biological tissues. *Ultrasonic Imaging* 13, 111–134.
- Pousson, M., Van Hoescke, J., Goubel, F., 1990. Changes in elastic characteristics of human muscle induced by eccentric exercise. *Journal of Biomechanics* 23, 343–348.
- Sandrin, L., Tanter, M., Catheline, S., Fink, M., 2002a. Shear modulus imaging using 2D transient elastography. *IEEE Transaction of Ultrasonic, Ferroelectric and Frequency Control* 49, 426–435.
- Sandrin, L., Tanter, M., Gennisson, J.L., Catheline, S., Fink, M., 2002b. Shear elasticity probe for soft tissues using 1D transient elastography. *IEEE Transaction of Ultrasonic, Ferroelectric and Frequency Control* 49, 436–446.
- Taylor, N.A., Sanders, R.H., Howick, E.I., Stanley, S.L., 1991. Static and dynamic assessment of the Biodex dynamometer. *European Journal of Applied Physiology* 62, 180–188.
- Winters, J., Starck, L., Seif-Naraghi, A.H., 1988. An analysis of the sources of musculo-skeletal system impedance. *Journal of Biomechanics* 21, 1011–1025.
- Yamakoshi, Y., Sato, J., Sato, T., 1990. Ultrasonic imaging of internal vibration of soft tissue under forced vibration. *IEEE Transaction of Ultrasonic, Ferroelectric and Frequency Control* 37, 45–53.
- Zahalak, G.I., Heyman, S.J., 1979. A quantitative evaluation of the frequency-response characteristics of active human skeletal muscle in vivo. *Journal of Biomechanical Engineering* 101, 28–37.
- Zee, M., Voigt, M., 2001. Moment dependency of the series elastic stiffness in the human plantar flexors measured in vivo. *Journal of Biomechanics* 34, 1399–1406.